Weldable, malleable and programmable epoxy vitrimers with high mechanical properties and water insensitivity

Hanchao Liu[1], Hao Zhang[1], Hao Wang, Xin Huang, Guangsu Huang[*], Jinrong Wu[*]

State Key Laboratory of Polymer Materials Engineering, College of Polymer Science and Engineering, Sichuan University, Chengdu 610065, China

HIGHLIGHTS

- A novel curing agent (TA) bearing imine backbones was synthesized conveniently.
- Epoxy vitrimers based on imine bond were fabricated by curing DGEBF with TA.
- Dynamic and high mechanical property of the vitrimer were simultaneously achieved.
- The vitrimer exhibited high water-resistance due to the network's hydrophobicity.

GRAPHICAL ABSTRACT
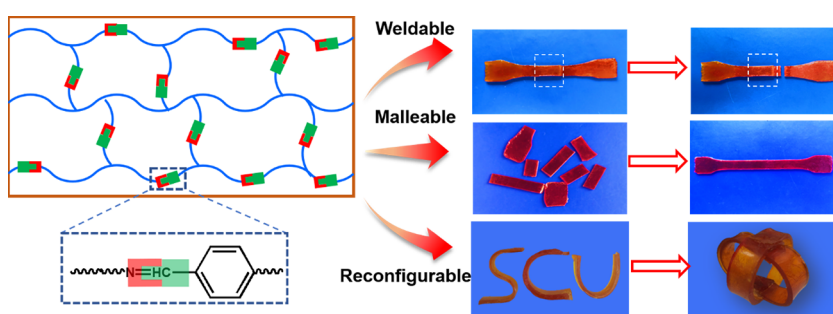
ARTICLE INFO

ABSTRACT

Vitrimers with covalent adaptable networks usually show low mechanical properties and water resistivity. Here, we report an epoxy vitrimer which possesses not only high weldability, malleability and programmability, but also outstanding mechanical properties and water insensitivity. Such epoxy vitrimer is fabricated by crosslinking diglycidyl ether of bisphenol F (DGEBF) with a novel curing agent bearing imine backbones and amino terminals. The curing agent is synthesized by a one-pot reaction between 3-aminobenzylamine and terephthalaldehyde by taking advantage of the different reactivity of the aromatic amine and aliphatic amine. The dynamic imine bonds of the curing agent enable malleability, shape reconfiguration and programming of the epoxy vitrimer, while the aromatic structure of the curing agent imparts the epoxy vitrimer with high tensile strength, Young modulus and thermal stability. Moreover, the epoxy vitrimer is highly water-resistant due to the hydrophobicity and high crosslinking density of the network. Such a combination of comprehensive properties and convenient fabrication approach makes the epoxy vitrimer hold great promise to serve as structural materials in diverse applications.

1. Introduction

As an important category of thermosets, epoxy resin shows high mechanical strength, modulus, thermal and dimensional stability, and easy processability, thus it is widely used as structural materials in various applications, such as aerospace vehicles, large passenger airliners, limousines, wind turbines and so on. Such applications usually expose epoxy resins to severe force and vibration conditions, thus easily generating mechanical damages like cracks and fractures in the structural materials. These damages if not repaired in time will substantially deteriorate the reliability and service lifetime of epoxy products, and even cause unexpected disasters. However, like many other thermosets,

---

epoxy resin is hard to be repaired because of its irreversible covalent networks. Even worse, the insoluble and infusible covalent networks do not allow epoxy to be reconfigured or recycled, resulting in a great waste of resources [1]. Therefore, it is highly desirable to develop mendable and recyclable epoxy.

A lot of efforts have been made to prepare malleable and recyclable thermosets by incorporating reversible bonds into the polymer networks [2–13]. For example, Diels-Alder (DA) reaction and cycloaddition of cinnamoyl groups have been utilized to design reversible networks [14–17]. However, such reversible networks cannot maintain their structural integrity and even start to flow at high temperature, as the dissociative mechanism of these reversible bonds leads to a sudden drop in viscosity of the materials [18]. Alternatively, "covalent adaptable networks" (CANs) [19–21] or "vitrimers" [22] based on associative exchange reactions exhibit similar reversible characteristics, while maintaining integral networks without much change in the number of chemical bonds and crosslinks even at elevated temperatures. In recent years, a number of reversible motifs, such as transesterification [23–27], alkoxyamine moieties [28], trithiocarbonate exchange [19], urethane exchange [20], vinylogous urethane transamidation [21], olefin metathesis [22], boronic ester exchange [29], thiol-Michael reaction [30], and carbonate exchange [31] have been utilized to construct vitrimers. Unfortunately, specific catalysts are required to initiate the exchange reactions in most cases, which may shorten the lifetime of vitrimers due to the possible catalyst quenching. For catalyst-free dynamic networks, sophisticated molecular designs for dynamic motifs, such as vinylogous urethane transamidation, to a large extent limit the extensive application of the vitrimers. Imine bond, which is formed by the reaction between amine and aldehyde, has the advantage of self-healing or recycling without catalyst and thus has been utilized to fabricate vitrimers based on various polymeric materials such as polyimines, polyimides, polybutadiene elastomers and gels, which exhibit recyclability and malleability [32–37]. However, two challenges still exist in these vitrimers: insufficient mechanical performance and water sensitivity [29–31,33,34]. For example, the tensile stress of polybutadiene crosslinked by imine linkages is lower than 6 MPa [36]. For the polyimine vitrimer, which is densely crosslinked by imine bonds, the tensile stress and Young modulus are lower than 45 MPa and 1500 MPa, respectively [33]. Even worse, due to the hydrolysis of imine bond, the mechanical property of the polyimine network decreases drastically after exposure to moisture [38]. These drawbacks will largely limit the applications of the vitrimers, especially for structural materials exposed to harsh conditions.

In this paper, we report a class of imine-bond crosslinked epoxy vitrimers, which possess not only high mechanical properties and water insensitivity, but also ideal weldability, recyclability and programmability. These epoxy vitrimers are fabricated by introducing a novel curing agent (TA) which bears imine bonds on the backbones and aromatic amines as terminals. Such curing agent is synthesized by a one-pot reaction between terephthalaldehyde (TAD) and 3-aminobenzylamine (AB), which does not involve any separation step by taking the advantage of the different reactivity between aliphatic and aromatic amine. After curing, the rigid structure of the curing agent and the high crosslinking density of the polymer network endow the vitrimers with high mechanical properties and water insensitivity, while the dynamic imine bonds enable weldability, reprocessability and programmability of the vitrimers. This work provides a new approach to design high-performance and catalyst-free malleable epoxies.

2. Experimental

2.1. Materials

Diglycidyl ether of bisphenol F (DGEBF) with an epoxy equivalent weight of 170 g (equiv)$^{-1}$ was purchased from Luohe Chemistry Co. Ltd., China. Terephthalaldehyde was purchased from Aldrich. 3-Aminobenzylamine was purchased from Aladdin®. All materials were used as received without further purification.

2.2. Preparation of imine curing agent

A certain amount of terephthalaldehyde (TAD) were dissolved in 500 mL of chloroform and mechanically stirred for 30 min. Then, a certain amount of 3-aminobenzylamine (AB) and 0.1 mol of $MgSO_4$ were added. The mixture was stirred for 24 h under room temperature. After filtration and evaporation, the curing agent with imine bonds, which is named as TA, can be got.

2.3. Preparation of epoxy vitrimers

A certain stoichiometric amount of imine curing agent was mixed with diglycidyl ether of bisphenol F (DGEBF). Then the mixture was mechanically stirred for 15 min before it was degassed in a vacuum oven at 60 °C for 1 h to remove air bubbles. Afterward, the degassed mixture was poured into a preheated PTFE mold and cured following the stepwise schedule: 80 °C for 3 h, 120 °C for 2 h, 150 °C for 3 h. Samples are denoted as EP-TA-m, where m refers to the stoichiometric ratio of the hydrogen on the amine group to the epoxy group on DGEBF. For example, EP-TA-1.5 refers to the sample cured by DGEBF and 1.5-fold excessive TA.

Control samples were prepared by curing DGEBF with AB by the same method. Samples were denoted as EP-AB-n, where n refers to the stoichiometric ratio of the hydrogen on the amine group to the epoxy group on DGEBF.

2.4. Characterization

Fourier transform infrared (FTIR) spectroscopy was performed on a Thermo Scientific Nicolet 6700 spectrometer in the range from 400 to 4000 cm^{-1} using KBr pellets. ^1H NMR spectra were collected using a Bruker AV-600 spectrometer (600 MHz) with CDCl$_3$ as the solvent. Dynamic mechanical analysis (DMA) experiments were conducted in a three-point bending mode using a DMA Q800 (TA instruments). All non-isothermal runs (temperature scans) were performed in the "multifrequency, strain" mode at 1 Hz, from 25 °C to 250 °C at a heating rate of 3 °C/min. The temperature where the maximum of the loss factor tanδ showed was evaluated as the glass transition temperature (T_g). With the same instrument, stress relaxation test was conducted. During the test, a sample was first equilibrated at a certain temperature for 15 min. Then an instantaneous 0.5% strain was applied to the sample within 2 s. Tensile measurement was conducted on a universal testing machine (Instron 5567, US) at room temperature with a cross-head speed of 1 mm/min. The thermal stability was measured by thermalgravimetric analysis (TG209F1, netzsch, Germany) under nitrogen atmosphere. The heating rate was 10 °C/min.

3. Results and discussion

3.1. Synthesis and characterization of the curing agent

To construct an epoxy vitrimer crosslinked with imine bonds, we first synthesize an amino-capped crosslinker bearing imine bonds. Such a crosslinker can be fabricated by reacting dialdehyde with excessive diamine. However, if the two amine groups on the diamine have the same reactivity, successive condensation between dialdehyde and diamine may take place, resulting in the formation of long-chain molecules with very poor solubility and high viscosity. Meanwhile, part of the diamine still remains unreacted, thus tedious separation and purification steps are indispensable to isolate the crosslinker from the unreacted diamine molecules. To address these issues, we develop a one-pot method to synthesize a curing agent bearing imine bonds (TA) utilizing terephthalaldehyde (TAD) to react with 3-aminobenzylamine
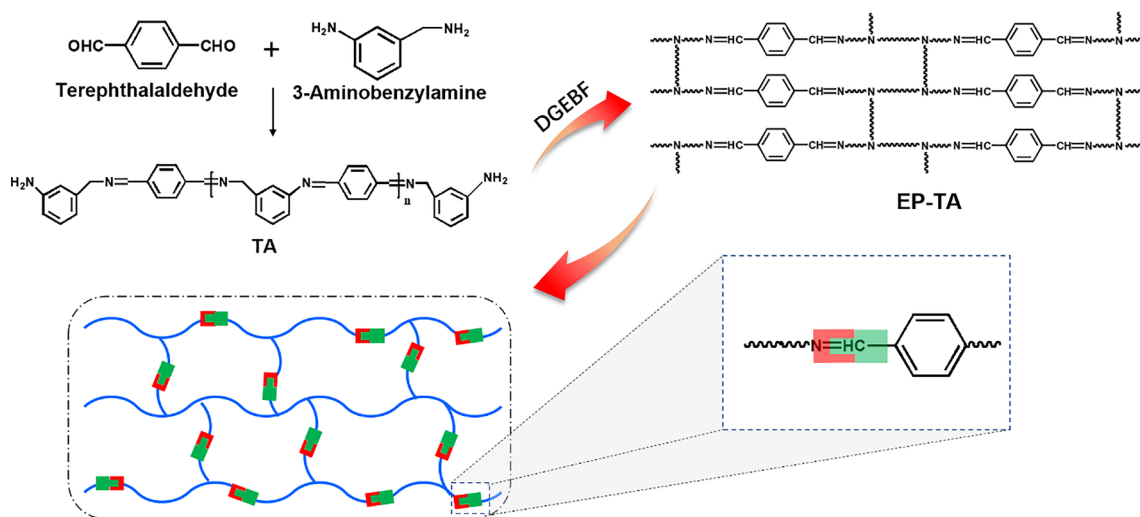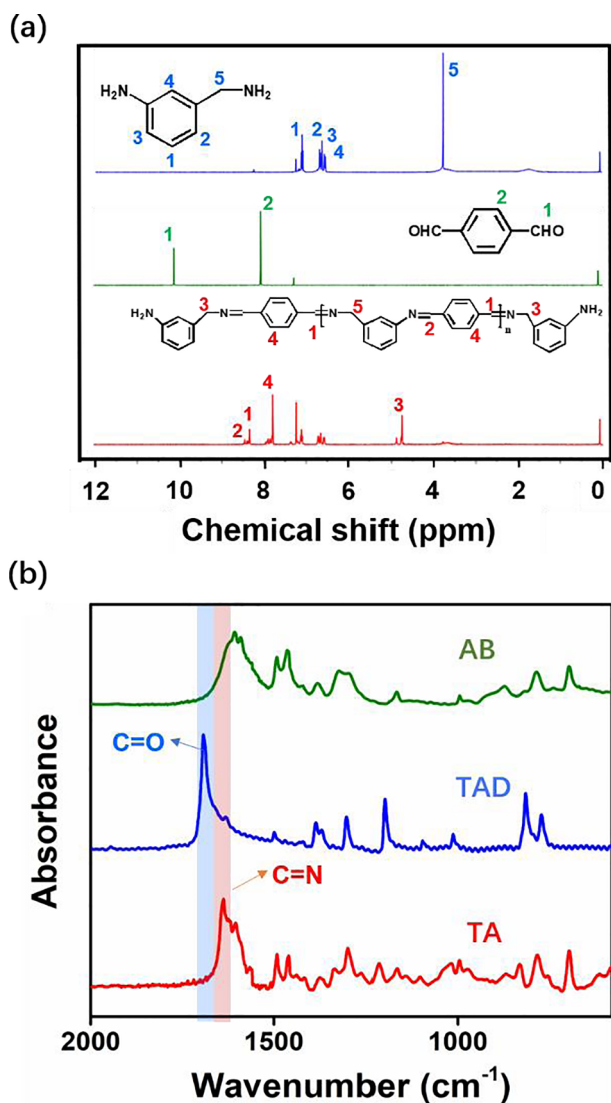
Fig. 1. Synthetic description of the TA and EP-TA.

(a)

(b)

Fig. 2. (a) ^{1}H NMR (b) and FTIR spectra of TA, TAD and AB.

(AB). Each AB molecule bears an aliphatic amine group and an aromatic amine group. The higher reactivity of aliphatic amine makes it much more prone to be consumed, generating products end capped with aromatic amino groups. However, although the lower reactivity of aromatic amine inhibits the formation of long-chain molecules to some extent, the successive condensation is inevitable, which will result in an increased ratio of AB/TAD as the reaction progresses. The offset of the ratio of AB/TAD further leads to the existence of residual AB in the products, which will result in the formation of inadaptable linkages after curing, decreasing the dynamic property of the crosslinking network. Thus, it is vital to tuning the ratio of AB/TAD to a proper value. By carefully adjusting the ratio of AB/TAD to 1.71 (Fig. S1), all the crosslinker molecules are end capped with aromatic amino groups (Fig. 1). ^{1}H NMR spectra shows that the typical proton signal at 10.20 ppm corresponding to –CHO on TAD disappears after reaction, while new signals at 8.22–8.51 ppm belonging to –N = CH– appear in TA (Fig. 2a), indicating that all the –CHO groups have converted into imine bonds. Meanwhile, the signal at 3.82 ppm corresponding to the –CH$_2$– adjacent to –NH$_2$ on AB disappears. Instead, new signals at 4.83–4.92 ppm corresponding to the –CH$_2$– neighboring imine bond on TA become prominent, confirming that all the aliphatic amine groups on AB have been consumed during the reaction. In addition, FTIR tests display that a new peak at 1625 cm^{-1} assigned to C=N stretching vibration of imine bond appears on the spectra of TA, accompanied by the disappearance of the absorption peak at 1700 cm^{-1} corresponding to C=O stretching vibration of TAD (Fig. 2b), further proving the formation of imine bonds in TA. Collectively, these results demonstrate that we have successfully synthesized the amino-capped curing agent bearing imine bonds. We can envision that during the curing process, the amine groups react with epoxy groups, leading to the formation of the polymer network connected by imine bonds (Fig. 1), which will impart the network with dynamic property. It should be pointed out that TA is a mixture of compounds with different molecular weight. In the mixture, all the molecules bearing imine backbones are terminated with aromatic amine. Thus, separation and purification steps are not needed.

3.2. Dynamic property of the EP-TA crosslinking network

The epoxy vitrimers are prepared by curing diglycidyl ether of bisphenol F (DGEBF) with the synthesized TA crosslinker (see Experimental section). The resulting samples are denoted as EP-TA-m, where m refers to the stoichiometric ratio of the hydrogens on the amine groups to the epoxy groups on DGEBF. In addition, control
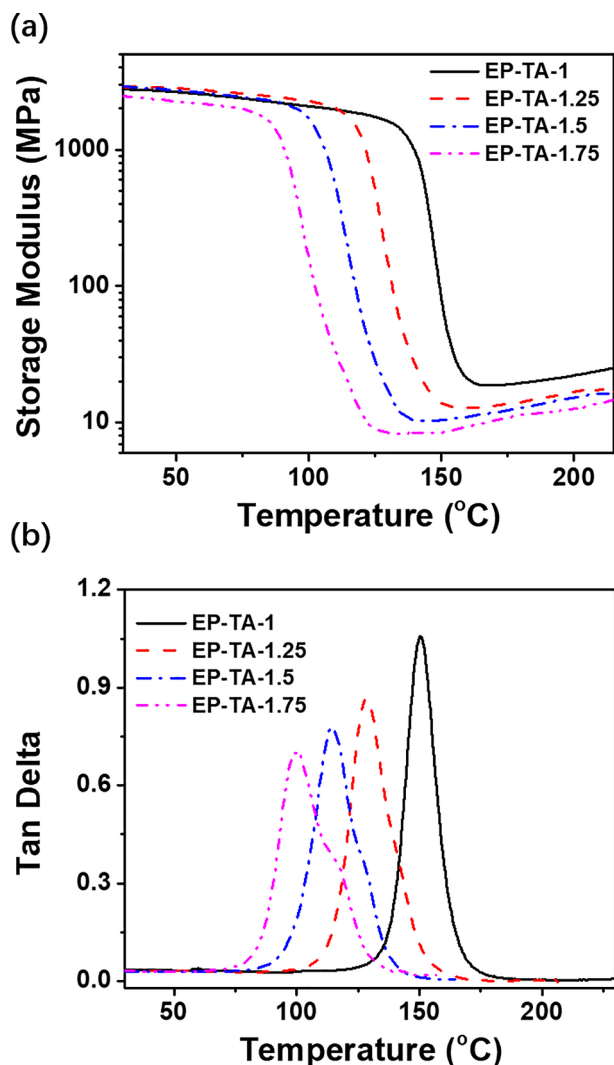
Fig. 3. Storage modulus (a) and tan δ (b) of EP-TA system.

Table 1
DMA results and thermal properties of EP-TA samples.

Sample	E_r (MPa) [a]	T_g (°C) [b]	T_i (°C) [c]	Char yield (wt%)[d]
EP-TA-1	19.22	150.3	312.4	31.81
EP-TA-1.25	13.83	128.4	303.7	35.13
EP-TA-1.5	10.46	113.51	301.0	36.79
EP-TA-1.75	8.42	100.2	298.4	37.97

[a] For EP-TA-1.75, the storage modulus between 125 and 145 °C is taken as the E_r value. For the other samples, the minimum of storage modulus at the rubber state is taken as the E_r value.
[b] The temperature of the maximum of the loss factor tanδ is assigned as the glass transition temperature.
[c] The thermal decomposition temperature at 5 wt% weight loss in an inert atmosphere.
[d] The char yield at 780 °C.

samples without imine bonds are prepared by crosslinking DGEBF with AB, and denoted as EP- AB-m, where m has the same meaning as the former one. After curing, each EP-TA sample shows a peak at 1625 cm^{-1} (Fig. S2), which is assigned to C=N stretching vibration of imine bond, indicating that imine bonds have been successfully introduced into the epoxy network. As the stoichiometric ratio of –NH– to epoxy group increases, the intensity of the peak at 1625 cm^{-1} increases, indicating more imine linkages in the network. The difference

in the loading of TA also leads to different network properties of EP-TA samples. DMA results show that as the stoichiometric ratio increases from 1 to 1.75, E_r decreases from 19.22 MPa to 8.42 MPa (Fig. 3a and Table 1), suggesting that the crosslinking density decreases upon the offset of stoichiometric balance. Meanwhile, the T_g decreases from 150.3 °C to 100.2 °C due to the decreased crosslinking density as the TA loading increases (Fig. 3b). However, compared with the inferior thermal properties of the epoxies cured with flexible curing cured with flexible curing agents [27,39,40], the T_g of EP-TA-1.75 still maintains at a relatively high temperature even though the TA is 1.75-fold excessive. Such a phenomenon can be attributed to the high rigidity of the TA molecules.

The dynamic properties of the EP-TA networks are investigated by stress relaxation test and compared with these of the EP-AB networks. During the relaxation test, each sample is first heated to a temperature 30 °C higher than T_g. Then, a strain of 0.5% is applied on the sample within 2 s and the relaxation modulus is monitored as a function of time. For EP-AB-1, barely no stress relaxation behavior can be observed (Fig. 4a). As the stoichiometric ratio of –NH– to epoxy group increases to 1.75, slight stress falloff appears, which is related to easier chain conformational changes due to the lower crosslinking density. By contrast, EP-TA samples show significant stress relaxation behavior due to the imine exchange (Fig. 4b). As the loading of TA increases, EP-TA samples exhibit much faster relaxation speeds and much lower equilibrium modulus, indicating a better dynamic property. During the curing process, reactions occur not only between epoxy and amine but also between epoxy and hydroxyl, especially at high temperature, which results in the formation of the inadaptable crosslinking (ether linkage). Thus, the equilibrium value of G/G$_0$ is relatively high when the stoichiometric ratio of –NH– to epoxy group is 1 (Fig. 4b). As the amount of TA increases, the abundance of amine suppresses the formation of ether linkage, which contributes to a more significant dynamic behavior of the crosslinking network (Fig. S2). Moreover, the residual primary amino groups also catalyze the exchanging reaction between imine bonds, leading to a more prominent and faster stress relaxation with lower equilibrium modulus [37].

Based on the Maxwell model for viscoelastic fluids, relaxation time is defined as the time needed to achieve G/G$_0$ = 0.37 [41,42]. As shown in Fig. 4c and d, the temperature dependence of the relaxation time of EP-TA-1.75 follows Arrhenius' law [41,42]. By contrast, the slight relaxation of EP-AB-1.75 does not show any temperature dependence (Fig. S3). According to Arrhenius' law,

$$\ln \tau = \ln \tau_0 + E_a/RT \qquad (1)$$

the activation energy of the vitrimer network is determined to be 61.94 kJ mol^{-1}. As the temperature rises, the adaptivity of the EP-TA-1.75 network is activated as a result of imine exchange. The topology freezing transition temperature (T_v), which corresponds to the transition from a solid to a viscous fluid, is defined as the temperature at which a viscosity of 10^{12} Pa·s is reached. According to the Maxwell relation:

$$\eta = G \cdot \tau* \qquad (2)$$

$$G = E'/(2(1 + \nu)) \qquad (3)$$

(ν: 0.5, the Poisson's ratio usually used for rubbery materials; E' is 8.42 MPa according to the DMA data), the hypothetical T_v thus obtained is 2.43 °C [43–47]. However, when the temperature is below T_g, the dynamic behavior of vitrimer is inhibited because the network is frozen by the lack of segmental motions. After the temperature rises above T_g, the fast exchange of the dynamic linkage leads to a fast relaxation of the EP-TA-1.75 network.
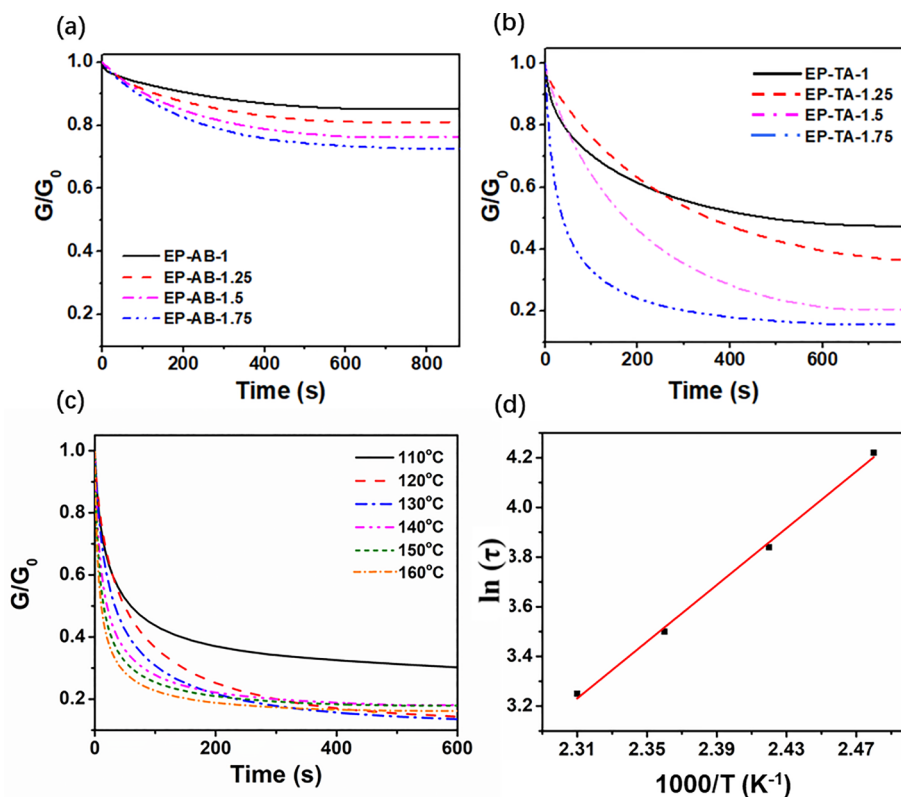
Fig. 4. Normalized stress-relaxation curves of (a) EP-AB samples and (b) EP-TA samples. (c) Normalized stress-relaxation curves of EP-TA-1.75 at different temperatures. (d) Fitting of the relaxation times to the Arrhenius equation.
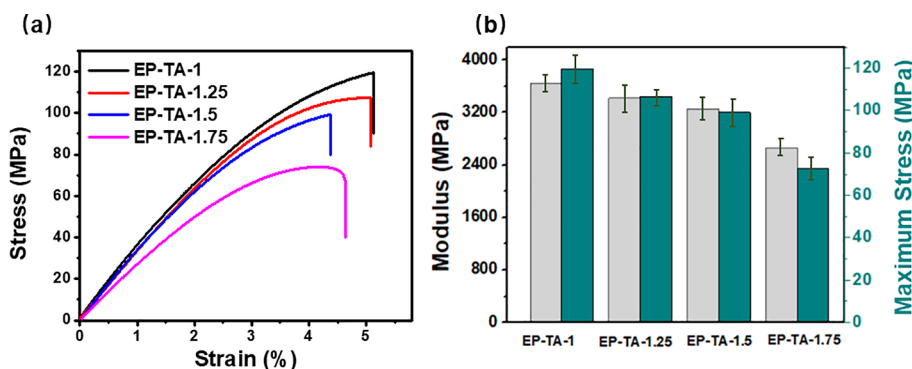

Fig. 5. Typical stress-strain curves (a) and mechanical properties (b) of EP-TA samples.

Table 2
Mechanical property of the virgin and welded EP-TA samples.

Sample	Stress (MPa) [a]	Strain (%) [a]	Stress (MPa) [b]	Strain (%) [b]	Healing efficiency (%) [c]
EP-TA-1	119.5	5.10	15.62	0.58	13.1
EP-TA-1.25	106.7	5.01	29.84	1.11	28.7
EP-TA-1.5	99.11	4.38	46.47	2.01	52.4
EP-TA-1.75	72.77	4.60	63.89	3.94	87.8

[a] The mechanical property of the virgin sample.
[b] The mechanical property of the welded sample.
[c] The healing efficiency is calculated based on the tensile stress of the virgin and welded samples.

3.3. Mechanical property, weldability, malleability and reconfigurability of EP-TA

Most malleable epoxy resins show quite low mechanical properties due to the low bond energy of dynamic bonds [27,40,48–54]. This drawback, however, can be overcome by using the TA crosslinker, since it bears many aromatic rings on the chain backbones, which can provide high rigidity to the polymer network. Indeed, results of tensile tests show that the tensile strength and Young modulus of EP-TA-1 are 119.5 MPa and 3636.5 MPa, respectively, exhibiting excellent mechanical properties (Fig. 5 and Table 2). As the TA loading increases, the mechanical properties decrease slowly due to the decreased crosslinking density. However, EP-TA-1.75 still possesses a tensile strength of 72.77 MPa and Young modulus of 2682.5 MPa, which are quite high compared with that of most reported epoxy vitrimers [27,40,48–54].

The dynamic imine bonds impart the EP-TA vitrimers with weldability and malleability. To investigate the weldability of EP-TA-1.75, a tensile specimen is cut into half and the two parts are overlapped by 10 mm. Before pressing the two parts together with a binder clip, one drop of diethylenetriamine solution in DMF solvent (10 mg·mL^{-1}) is added to the overlapped position to accelerate the imine exchange reaction [35]. After being heated under 140 °C for 1 h, the two halves are
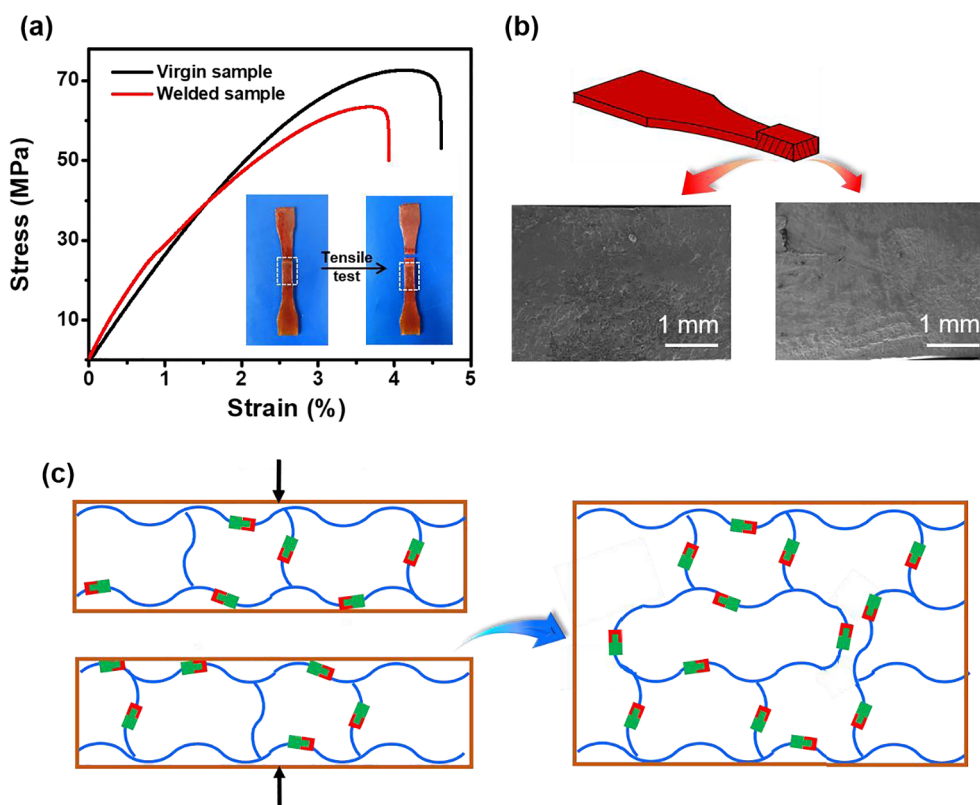
Fig. 6. (a) Typical stress-strain curves of the virgin sample and welded sample. (b) SEM images of the side view and section of the overlapped part after welding. (c) Schematic description of the welding process based on imine exchange.

welded tightly due to the exchange reaction between imine bonds (Fig. 6c). As shown in Fig. 6a, the welded sample fractures at a different place from the originally healed position during the tensile test. The overlapped area is not separated during the whole tensile process. Meanwhile, the welded sample can sustain a tensile stress of 63.89 MPa (Fig. 6a), which is 87.8% of that of the virgin sample. Though the mechanical performance is reduced to a certain degree due to the decreased crosslinking density induced by the exchange between diethylenetriamine and the imine bonds in the network, the healing efficiency is quite acceptable [35]. The weldability of the sample is also investigated by SEM (Fig. 6b). The side and section views of the overlapped region after healing exhibit no gap between the two parts, indicating that the sample is ideally welded together. The weldability of other EP-TA samples is also investigated. As the crosslinking density increases, the healing efficiency decreases stepwise (Table 2). For EP-TA-1, the healing efficiency is only 13.1%. There are two reasons for such a low healing efficiency: first, the network is still in frozen state when the T_g is higher than the welding temperature; second, a higher content of the inadaptable crosslinking exists in the network due to the lower loading of TA.

When catastrophic damage happens, the fractured EP-TA fragments can be reprocessed into integrated samples. To demonstrate this, we crush EP-TA-1.75 samples into small pieces and remold the pieces under 5 MPa at 140 °C. After hot press a recycled sample of full integrity can be obtained (Fig. 7a). The recycled sample is subjected to tensile testing and the result is compared with that of the original sample. As shown in Fig. 7a, as the heat-pressing time increases to 60 min, the healing efficiency reaches the maximum due to the sufficient bond exchanging reaction. Thus, 60 min is taken as optimum time length for heat-pressing. As shown in Fig. 7b, the average strength, Young modulus and elongation at break of the reprocessed sample are 74.6%, 80.3% and 60.8% of those of the virgin sample, respectively, demonstrating a good healing efficiency of EP-TA-1.75. Like many other

vitrimers, the healing of EP-TA is accompanied by the reduction of mechanical properties due to the simultaneous fracture of the irreversible bonds [18,36]. However, compared with other healable materials which possess high healing efficiency but are not robust enough for practical applications [27,47,52,53], the EP-TA vitrimers exhibit quite high healing efficiency without sacrificing the mechanical performances, which makes it highly competitive in fields where structural healable materials are needed.

The weldability and reconfigurability of the epoxy vitrimer derived from the dynamic imine bonds facilitate the reprocessing and programming of the cured materials without using moulds. As shown in Fig. 8, stripes of EP-TA-1.75 can be processed into various 3D structures by welding and deforming. For example, by welding several vitrimer stripes layer by layer with drops of diethylenetriamine solution in DMF solvent (10 mg·mL^{-1}), a vitrimer "brick" can be got (Fig. 8b). Moreover, due to the exchange between imine bonds, permanent deformation can be realized under external force. As such, the cured samples can be made into different patterns. We deform three vitrimer stripes into different shapes under 130 °C and keep the deformation for 20 min. After the force is removed, the deformation is maintained because of the adaptivity of the imine containing network, by which a pattern of digital numbers can be got (Fig. 8c). By the same method, the reconfiguring can be repeated: the numbers are then permanently deformed into another pattern under 130 °C. Further, if we combine the weldability and reconfigurability of the vitrimers, more complicated and elaborate 3D structures can be constructed. For example, four stripes of EP-TA-1.75 are bended at 130 °C and the ends of the stripes are welded together. Then we can get a cage-like structure (Fig. 8e). Considering the intrinsic shape memory property of epoxy resin, we envision that by utilizing reconfigurability and the shape memory property, complicated shape programming can be designed either reversibly or permanently on one vitrimer sample just by tuning the deforming temperature. As shown in Fig. 8(i) (iii) (iv) (v), two stripes are
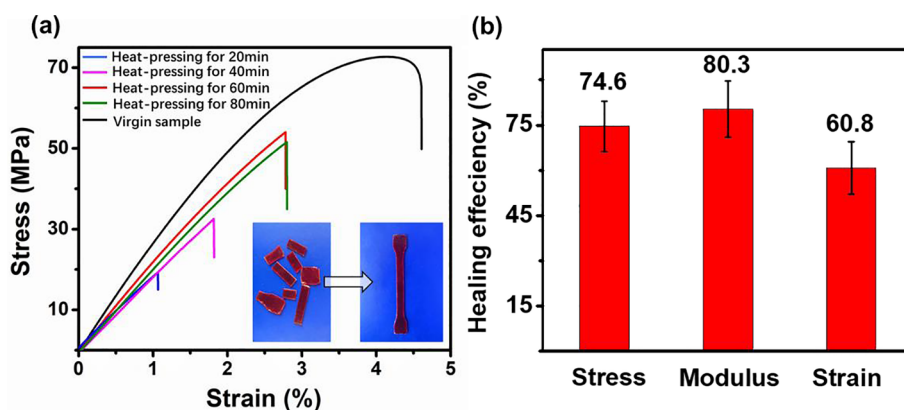
Fig. 7. (a) Typical stress-strain curves of virgin and reprocessed sample after heat-pressing for different time length. (b) The mechanical healing efficiency of the reprocessed EP-TA-1.75 after heat-pressing for 60 min.

welded together and bended into a cube under 120 °C. Straight after, the sample is cooled down to room temperature and the deformation is fixed. When the temperature is raised to 140 °C, the deformation is fully recovered and the original shape of the vitrimer can be got. Because the exchange between imine bonds is not fast enough when the temperature is 120 °C (Fig. 4), permanent shape change is hard to happen during the short period of time for shape changing. After the sample is cooled down to room temperature, the as-formed cube shape is temporarily fixed due to the elastic energy storage derived from the frozen of the polymer chains. When the temperature is raised to 140 °C, the temporary shape gradually recovers to the original shape due to the release of the elastic energy. However, if the deformation of the vitrimer is implemented at 140 °C, after one hour, a permanent shape change can be got due to the adaptivity of the network (Fig. 8(i) and (ii)). Thus, the shape and structure design of the vitrimers can be realized simply by welding and reconfiguring under different temperatures, which significantly simplifies the fabricating process and promotes the versatility of the material.

The low hypothetical T_v of 2.43 °C of EP-TA-1.75 indicates a high exchanging activity of the imine-containing network. Thus, this vitrimer may be potential for shape programming at much lower temperature rather than temperature above T_g. Considering the lack of segmental motion highly restricts the bond exchange at temperature below T_g, we first swell the vitrimer to "unfreeze" the frozen network. As shown in Fig. 8f and g, after being fully swelled in chloroform, the EP-TA-1.75 stripe is deformed into a "C" shape and allowed to dry at 40 °C under the deformation state. After the solvent is completely evaporated (the weight of the swelled stripe is constant), the external force is removed and the vitrimer shows no shape recovery. To examine whether the deformation is permanent, the vitrimer is heated above T_g. As expected, the new shape is almost stable except for a tiny shape change derived from the elastic recovery, indicating that the low T_v endows the vitrimer with the capacity of permanently deforming to new structures without the need of high temperature.

3.4. Water sensitivity and thermal stability of EP-TA

Due to the hydrolysis of imine bond, water sensitivity is a great challenge for imine containing networks. In order to investigate the water sensitivity of EP-TA-1.75, we immerse several samples in
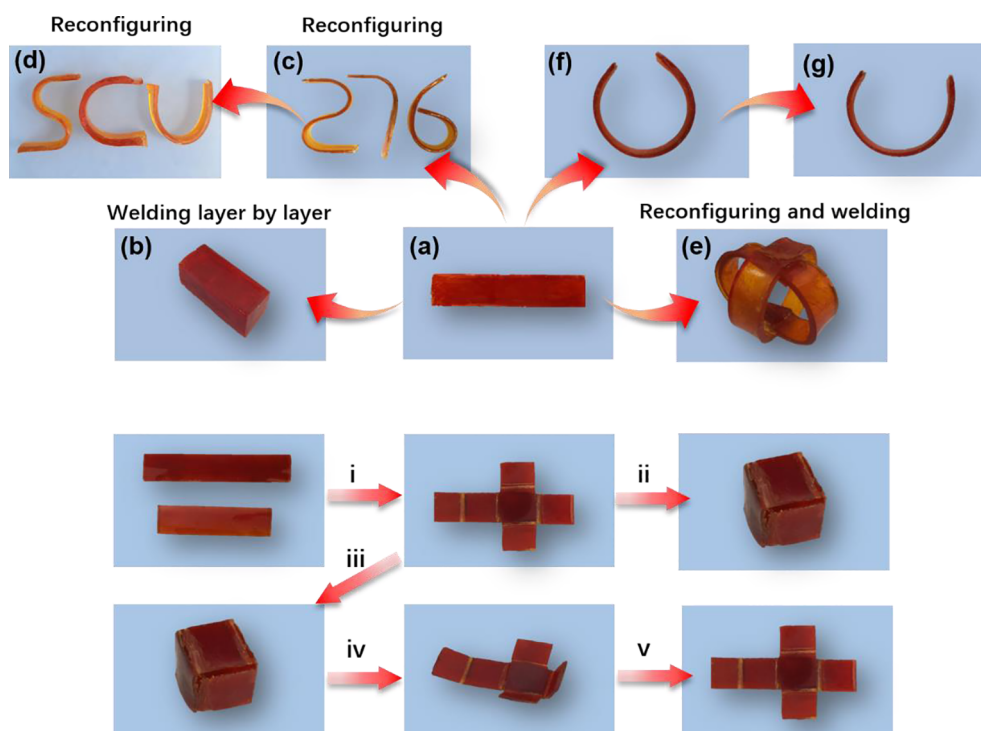

Fig. 8. Shape programming of EP-TA-1.75. (a) A vitrimer stripe. (b) A vitrimer brick fabricated by welding vitrimer stripes layer by layer. (c) (d) Reconfiguring vitrimer stripes into digital numbers and then reconfiguring the numbers into a "SCU" pattern. (e) A cage fabricated by reconfiguring and welding vitrimer stripes. (f) Swelling the vitrimer stripe in CHCl₃ and deforming the swelled sample, then keeping the deformation at 45 °C to remove the solvent. (g) Heating to 130 °C and the sample exhibits permanent deformation. (i) Welding two vitrimer stripes together. (iii) Deforming the welded stripes into a cube under 120 °C and then cooling down to room temperature while maintaining the deformation. (iv), (v) Rising the temperature to 140 °C and the vitrimer recovers to its original shape. (ii) Deforming the welded stripes into a cube under 140 °C and maintaining the deformation for 1 h at 140 °C. The deformation does not recover.
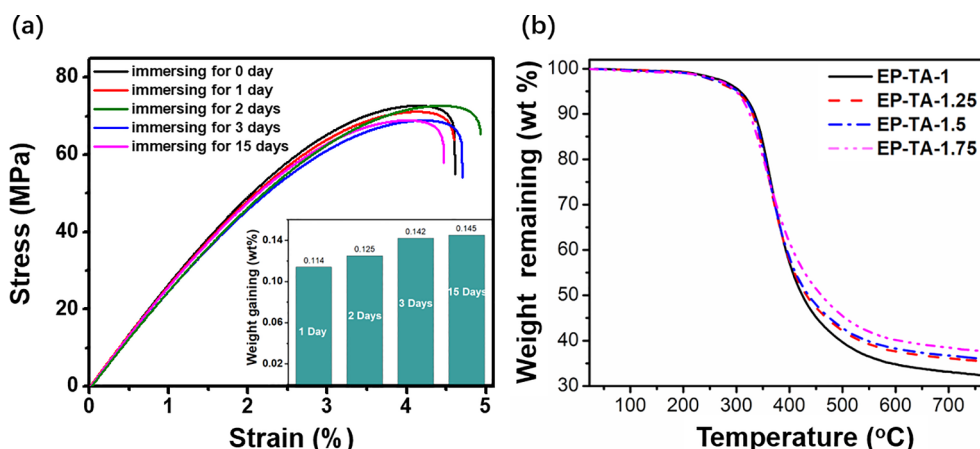
Fig. 9. (a) Typical stress-strain curve and weight gaining of EP-TA-1.75 after immersed in water for different times. (b) The thermogravimetric curve of EP-TA samples.

Table 3
The weight gaining and mechanical properties of EP-TA-1.75 after immersed in water for different times.

Immersing time (day)	0	1	2	3	15
Weight gaining (wt%)	0	0.114	0.125	0.142	0.145
Stress (MPa)	72.77	71.14	72.65	69.81	68.96
Young Modulus (MPa)	2682.5	2675.6	2485.2	2507.1	2637.6
Strain at break (%)	4.60	4.59	4.93	4.70	4.46

deionized water at room temperature for different periods of time and measure the weight increase of each sample. As shown in the inset of Fig. 9a and Table 3, as the immersing time in water increases from 1 day to 15 days, the weight gaining of the vitrimer sample increases slowly. However, the weight gaining is lower than 0.15%, which is negligible compared with that of the polyimine that is reported previously [38]. Moreover, the mechanical property of the samples after soaking for different periods of time barely changes compared with that of the virgin sample (Fig. 9a), which is in a sharp contrast with the tremendous decrease of the mechanical performance of polyimine network, indicating the excellent water insensitivity of EP-TA [38]. Although imine bond is prone to be hydrolyzed in the presence of water, which results in a high absorption of water of polyimine even though the material exhibits high T_g and crosslinking density, the EP-TA system possesses excellent water insensitivity, which can be attributed to the frozen and hydrophobic epoxy network [38].

It is worth noting that due to the dynamic nature of the exchangeable bonds, vitrimers can be degraded under certain circumstances [27,37,47,55,56]. We grind EP-TA-1.75 into powder, and add it into a vial containing diethylenetriamine solution in DMF solvent (10 mg·mL^{-1}). After being heated for 5 h at 140 °C, the vial is cooled down to room temperature and the residue is collected, dried and weighed. As shown in Fig. S4, the residue is 13.39% of the weight of the virgin powder. However, compared with many vitrimers [37,47,55], EP-TA-1.75 needs much harsher conditions to be degraded, which means the stability of the vitrimer is acceptable. Thus, considering the high mechanical property and the low sensitivity to water of EP-TA, we think that this vitrimer can be a good candidate for recyclable structural material under non-extreme conditions.

The thermal stability of the EP-TA system is investigated by thermal gravimetric analysis. As shown in Fig. 9b and Table 1, the initial decomposition temperature (T_i) at which the 5 wt% weight loss occurs decreases as the TA loading increases, due to the lower crosslinking density when the TA is excessive. However, due to the rigid structure of the TA containing network, even the curing agent is 1.75-fold excess, the T_i can still reach 298.4 °C, which is higher than that of the pure

polyimine network [35]. The char yield increases from 31.81 wt% to 37.97 wt% as the TA loading increases from 1 to 1.75-fold, which is attributed to the increasing amount of aromatic ring structure [35,54].

4. Conclusion

We prepare epoxy vitrimers based on dynamic imine bond by curing diglycidyl ether of bisphenol F (DGEBF) with a novel cuing agent synthesized by terephthalaldehyde and 3-aminobenzylamine in a simple way. Taking advantage of the different reactivity of the aromatic amine and aliphatic amine, the curing agent is synthesized by a one-pot reaction without any separation or purification step. Using the curing agent to crosslink DGEBF generates epoxy vitrimers, of which the dynamic imine linkages enable malleability, shape reconfiguration and programming, while the aromatic structure imparts the epoxy vitrimers with high tensile strength, Young modulus and thermal stability. The welded and remoulded samples exhibit healing efficiencies of 87.8% and 74.6%, respectively, and the complex shape programming can be realized by harnessing the shape reconfiguring property and shape memory property. Meanwhile, the tensile stress and Young modulus of the vitrimer are higher than 70 MPa and 2600 MPa, demonstrating a superior mechanical property compared with many reported vitrimers. Moreover, the epoxy vitrimer is highly water-resistant due to the hydrophobicity and high crosslinking density of the network. This approach may provide some new insights in the design of the easily prepared and catalyst-free recyclable epoxies, of which the combination of comprehensive properties makes them potential candidates for applications in structural materials.

Acknowledgements

Appendix A. Supplementary data

^{1}H NMR of TA with different AB/TAD values (Fig. S1); FTIR spectra of the cured EP-TA samples (Fig. S2); normalized stress-relaxation curves of EP-AB-1.75 at different temperatures (Fig. S3); photographs of EP-TA-1.75 powder before and after degradation in DMF solution of diethylenetriamine (Figure S4). Supplementary data to this article can be found online at https://doi.org/10.1016/j.cej.2019.02.177.

References

[1] C.J. Kloxin, T.F. Scott, B.J. Adzima, C.N. Bowman, Covalent adaptable networks

(CANs): a unique paradigm in cross-linked polymers, Macromolecules 43 (2010) 2643–2653, https://doi.org/10.1021/ma902596s.

[2] R.J. Wojtecki, M.A. Meador, S.J. Rowan, Using the dynamic bond to access macroscopically responsive structurally dynamic polymers, Nat. Mater. 10 (2011) 14–27, https://doi.org/10.1038/nmat2891.

[3] C.J. Kloxin, C.N. Bowman, Covalent adaptable networks: smart, reconfigurable and responsive network systems, Chem. Soc. Rev. 42 (2013) 7161–7173, https://doi.org/10.1039/C3CS60046G.

[4] X. Huang, M.J. Bolen, N.S. Zacharia, Silver nanoparticle aided self-healing of polyelectrolyte multilayers. PCCP 16 (2014) 10267–10273, https://doi.org/10.1039/C4CP00349G.

[5] N. Zheng, J. Hou, Y. Xu, Z. Fang, W. Zou, Q. Zhao, T. Xie, Catalyst-free thermoset polyurethane with permanent shape reconfigurability and highly tunable triple-shape memory performance, ACS Macro Lett. 6 (2017) 326–330, https://doi.org/10.1021/acsmacrolett.7b00037.

[6] Mengmeng Cui, Ngoc A. Nguyen, Peter V. Bonnesen, David Uhrig, Jong K. Keum, Rigid oligomer from lignin in designing of tough, Self-Healing, ACS Macro Lett. 7 (2018) 1328–1332, https://doi.org/10.1021/acsmacrolett.8b00600.

[7] Y. Wang, Y. Pan, Z. Zheng, X. Ding, Reconfigurable and reprocessable thermoset shape memory polymer with synergetic triple dynamic covalent bonds, Macromol. Rapid Commun. 39 (2018) 1800128, https://doi.org/10.1002/marc.201800128.

[8] X. Chen, M.A. Dam, K. Ono, A. Mal, H. Shen, S.R. Nutt, K. Sheran, F. Wudl, A thermally re-mendable cross-linked polymeric material, Science 295 (2002) 1698–1702, https://doi.org/10.1126/science.1065879.

[9] Y. Amamoto, H. Otsuka, A. Takahara, K. Matyjaszewski, Self-healing of covalently cross-linked polymers by reshuffling thiuram disulfide moieties in air under visible light, Adv. Mater. 24 (2012) 3975–3980, https://doi.org/10.1002/adma.201201928.

[10] C. Yuan, M.Z. Rong, M.Q. Zhang, Z.P. Zhang, Y.C. Yuan, Self-healing of polymers via synchronous covalent bond fission/radical recombination, Chem. Mater. 23 (2011) 5076–5081, https://doi.org/10.1021/cm202653w.

[11] J. Ling, M.Z. Rong, M.Q. Zhang, Photo-stimulated self-healing polyurethane containing dihydroxyl coumarin derivatives, Polymer 53 (2012) 2691–2698, https://doi.org/10.1016/j.polymer.2012.04.016.

[12] G. Deng, C. Tang, F. Li, H. Jiang, Y. Chen, Covalent cross-linked polymer gels with reversible sol-gel transition and self-healing properties, Macromolecules 43 (2010) 1191–1194, https://doi.org/10.1021/ma9022197.

[13] M. Pepels, I. Filot, B. Klumperman, H. Goossens, Self-healing systems based on disulfide-thiol exchange reactions, Polym. Chem. 4 (2013) 4955–4965, https://doi.org/10.1039/C3PY00087G.

[14] D.H. Turkenburg, H.R. Fischer, Diels-Alder based, thermo-reversible cross-linked epoxies for use in self-healing composites, Polymer 79 (2015) 187–194, https://doi.org/10.1016/j.polymer.2015.10.031.

[15] Kim K. Oehlenschlaeger, Jan O. Mueller, Josef Brandt, Stefan Hilf, Albena Lederer, Manfred Wilhelm Robert Graf, Michelle L. Coote, Friedrich G. Schmidt, Christopher Barner-Kowollik, Adaptable hetero Diels-Alder networks for fast self-healing under mild conditions, Adv. Mater. 26 (2014) 3561–3566, https://doi.org/10.1002/adma.201306258.

[16] P.A. Pratama, M. Sharifi, A.M. Peterson, G.R. Palmese, Room temperature self-healing thermoset based on the Diels-Alder reaction, ACS Appl. Mater. Interfaces 5 (2013) 12425–12431 10.1021/am403459e.

[17] C.M. Chung, Y.S. Roh, S.Y. Cho, J.G. Kim, Crack healing in polymeric materials via photochemical [2 + 2] cycloaddition, Chem. Mater. 16 (2004) 3982, https://doi.org/10.1021/cm049394+.

[18] M. Qiu, S. Wu, S. Fang, Z. Tang, B. Guo, Sustainable, recyclable and robust elastomers enabled by exchangeable interfacial cross-linking, J. Mater. Chem. A 6 (2018) 13607–13612, https://doi.org/10.1039/C8TA04173C.

[19] Y. Amamoto, J. Kamada, H. Otsuka, A. Takahara, K. Matyjaszewski, Repeatable photoinduced self-healing of covalently cross-linked polymers through reshuffling of trithiocarbonate units, Angew. Chem. Int. Ed. 50 (2011) 1660–1663, https://doi.org/10.1002/anie.201003888.

[20] D.J. Fortman, J.P. Brutman, C.J. Cramer, M.A. Hillmyer, W.R. Dichtel, Synthesis and testing of a zinc amide self-healing system and a boronic ester vitrimer system, J. Am. Chem. Soc. 137 (2015) 14019–14022, https://doi.org/10.1021/jacs.5b08084.

[21] W. Denissen, G. Rivero, R. Nicolay, L. Leibler, J.M. Winne, F.E. Du Prez, Vinylogous urethane vitrimers, Adv. Funct. Mater. 25 (2015) 2451–2457, https://doi.org/10.1002/adfm.201404553.

[22] Y.X. Lu, F. Tournilhac, L. Leibler, Z. Guan, A new reagent for direct difluoromethylation, J. Am. Chem. Soc. 134 (2012) 8424–8427, https://doi.org/10.1021/ja303356z.

[23] Z. Yang, Q. Wang, T. Wang, Dual-triggered and thermally reconfigurable shape memory graphene-vitrimer composites, ACS Appl. Mater. Interfaces 8 (2016) 21691–21699, https://doi.org/10.1021/acsami.6b07403.

[24] L. Lu, J. Fan, G. Li, Intrinsic healable and recyclable thermoset epoxy based on shape memory effect and transesterification reaction, Polymer 105 (2016) 10–18, https://doi.org/10.1016/j.polymer.2016.10.013.

[25] Lu. Lu, Jian Pan, Guoqiang Li, Recyclable high-performance epoxy based on transesterification reaction, J. Mater. Chem. A 5 (2017) 21505–21513, https://doi.org/10.1039/C7TA06397K.

[26] F.I. Altuna, C.E. Hoppe, R.J.J. Williams, Epoxy vitrimers: the effect of transesterification reactions on the network structure, Polymers 10 (2018) 43, https://doi.org/10.3390/polym10010043.

[27] T. Liu, C. Hao, L. Wang, Y. Li, W. Liu, J. Xin, J. Zhang, Eugenol-derived biobased epoxy: shape memory, repairing, and recyclability, Macromolecules 50 (2017) 8588–8597, https://doi.org/10.1021/acs.macromol.7b01889.

[28] C.E. Yuan, M.Q. Zhang, M.Z. Rong, Application of alkoxyamine in self-healing of epoxy, J. Mater. Chem. A 2 (2014) 6558–6566, https://doi.org/10.1039/C4TA00130C.

[29] O.R. Cromwell, J. Chung, Z. Guan, Mechanically activated, catalyst-free polyhydroxyurethane vitrimers, J. Am. Chem. Soc. 137 (2015) 6492–6495, https://doi.org/10.1021/jacs.5b08084.

[30] B. Zhang, Z.A. Digby, J.A. Flum, P. Chakma, J.M. Saul, J.L. Sparks, D. Konkolewicz, Dynamic thiol-michael chemistry for thermoresponsive rehealable and malleable networks, Macromolecules 49 (2016) 6871–6878, https://doi.org/10.1021/acs.macromol.6b01061.

[31] R.L. Snyder, D.J. Fortman, G.X. De Hoe, M.A. Hillmyer, W.R. Dichtel, Reprocessable acid-degradable polycarbonate vitrimers, Macromolecules 51 (2018) 389–397, https://doi.org/10.1021/acs.macromol.7b02299.

[32] H. Li, J. Bai, Z. Shi, J. Yin, Environmental friendly polymers based on schiff-base reaction with self-healing, remolding and degradable ability, Polymer 85 (2016) 106–113, https://doi.org/10.1016/j.polymer.2016.01.050.

[33] P. Taynton, K. Yu, R.K. Shoemaker, Y. Jin, H.J. Qi, W. Zhang, Heat-or water-driven malleability in a highly recyclable covalent network polymer, Adv. Mater. 26 (2014) 3938–3942, https://doi.org/10.1002/adma.201400317.

[34] Philip Taynton, Huagang Ni, Chengpu Zhu, Yu. Kai, Samuel Loob, H. Yinghua Jin, Jerry Qi, Wei Zhang, Repairable woven carbon fiber composites with full recyclability enabled by malleable polyimine networks, Advanced Materials 28 (2016) 2904–2909 10.1002/adma.201505245.

[35] X. Lei, Y. Jin, H. Sun, W. Zhang, Rehealable imide-imine hybrid polymers with full recyclability, J. Mater. Chem. A 5 (2017) 21140–21145, https://doi.org/10.1039/C7TA07076D.

[36] Huan Zhang, Dong Wang, Wenxing Liu, Pengchong Li, Jiajian Liu, Chenyang Liu, Jiawei Zhang Ning Zhao, Xu Jian, Recyclable polybutadiene elastomer based on dynamic imine bond, J. Polym. Sci. Part A: Polym. Chem. 55 (2017) 2011–2018, https://doi.org/10.1002/pola.28577.

[37] A. Chao, I. Negulescu, D. Zhang, Dynamic covalent polymer networks based on degenerative imine bond exchange: tuning the malleability and self-healing properties by solvent, Macromolecules 49 (2016) 6277–6284, https://doi.org/10.1021/acs.macromol.6b01443.

[38] P. Taynton, C. Zhu, S. Loob, R. Shoemaker, J. Pritchard, Y. Jin, W. Zhang, Rehealable polyimine thermosets: polymer composition and moisture sensitivity, Polym. Chem. 7 (2016) 7052–7056, https://doi.org/10.1039/C6PY01395C.

[39] N. Tian, R. Ning, J. Kong, Self-toughening of epoxy resin through controlling topology of cross-linked networks, Polymer 99 (2016) 376–385, https://doi.org/10.1016/j.polymer.2016.07.038.

[40] Y. Yang, E.M. Terentjev, Y. Wei, Y. Ji, Solvent-assisted programming of flat polymer sheets into reconfigurable and self-healing 3D structures, Nat. Commun. 9 (2018) 1906, https://doi.org/10.1038/s41467-018-04257-x.

[41] M. Capelot, D. Montarnal, F. Tournilhac, L. Leibler, Metal-catalyzed transesterification for healing and assembling of thermosets, J. Am. Chem. Soc. 134 (2012) 7664–7667, https://doi.org/10.1021/ja302894k.

[42] M. Capelot, M.M. Unterlass, F. Tournilhac, L. Leibler, Catalytic control of the vitrimer glass transition, ACS Macro Lett. 1 (2012) 789–792, https://doi.org/10.1021/mz300239f.

[43] M.A.J. Van der Mee, R.M.A. l'Abee, G. Portale, J.G.P. Goossens, M. Van Duin, Synthesis, structure, and properties of ionic thermoplastic elastomers based on maleated ethylene/propylene copolymers, Macromolecules 41 (2008) 5493–5501, https://doi.org/10.1021/ma8007509.

[44] J.P. Brutman, P.A. Delgado, M.A. Hillmyer, Polylactide vitrimers, ACS Macro Lett. 3 (2014) 607–610, https://doi.org/10.1021/mz500269w.

[45] W. Denissen, G. Rivero, R. Nicola, L. Leibler, J.M. Winne, F.E. Du Prez, Vinylogous urethane vitrimers, Adv. Funct. Mater. 25 (2015) 2451–2457, https://doi.org/10.1002/adfm.201404553.

[46] M.M. Obadia, B.P. Mudraboyina, A. Serghei, D. Montarnal, E. Drockenmuller, Reprocessing and recycling of highly cross-linked ion-conducting networks through transalkylation exchanges of C-N bonds, J. Am. Chem. Soc. 137 (2015) 6078–6083, https://doi.org/10.1021/jacs.5b02653.

[47] Z. Ma, Y. Wang, J. Zhu, J. Yu, C. Hu, Bio-based epoxy vitrimers: reprocessibility, controllable shape memory, and degradability, J. Polym. Sci., Part A: Polym. Chem. 55 (2017) 1790–1799, https://doi.org/10.1002/pola.28544.

[48] A. Legrand, C. Soulié-Ziakovic, Silica-epoxy vitrimer nanocomposites, Macromolecules 49 (2016) 5893–5902, https://doi.org/10.1021/acs.macromol.6b00826.

[49] F. Zhou, Z. Guo, W. Wang, X. Lei, B. Zhang, H. Zhang, Q. Zhang, Preparation of self-healing, recyclable epoxy resins and low-electrical resistance composites based on double-disulfide bond exchange, Compos. Sci. Technol. 167 (2018) 79–85, https://doi.org/10.1016/j.compscitech.2018.07.041.

[50] J. Han, T. Liu, C. Hao, S. Zhang, B. Guo, J. Zhang, A catalyst-free epoxy vitrimer system based on multifunctional hyperbranched polymer, Macromolecules 51 (2018) 6789–6799, https://doi.org/10.1021/acs.macromol.8b01424.

[51] X. Wu, X. Yang, R. Yu, X.J. Zhao, Y. Zhang, W. Huang, A facile access to stiff epoxy vitrimers with excellent mechanical properties via siloxane equilibration, J. Mater. Chem. A 6 (2018) 10184–10188, https://doi.org/10.1039/C8TA02102C.

[52] L. Zhou, G. Zhang, Y. Feng, H. Zhang, J. Li, X. Shi, Design of a self-healing and flame-retardant cyclotriphosphazene-based epoxy vitrimer, J. Mater. Sci. 53 (2018) 7030–7047, https://doi.org/10.1007/s10853-018-2015-z.

[53] Q. Shi, K. Yu, M.L. Dunn, T. Wang, H.J. Qi, Solvent assisted pressure-free surface welding and reprocessing of malleable epoxy polymers, Macromolecules 49 (2016) 5527–5537, https://doi.org/10.1021/acs.macromol.6b00858.

[54] Qian Shi, Kai Yu, Xiao Kuang, Xiaoming Mu, K. Conner, B. Dunn, L. Martin, D. Dunn, Tiejun Wang, H. Jerry Qi, Recyclable 3D printing of vitrimer epoxy, Mater.

Horiz. 4 (2017) 598–607, https://doi.org/10.1039/C7MH00043J.

[55] A.R. de Luzuriaga, R. Martin, N. Markaide, A. Rekondo, G. Cabañero, J. Rodríguez, I. Odriozola, Epoxy resin with exchangeable disulfide crosslinks to obtain re-processable, repairable and recyclable fiber-reinforced thermoset composites, Mater. Horiz. 3 (2016) 241–247, https://doi.org/10.1039/C6MH00029K.

[56] X. Kuang, Y. Zhou, Q. Shi, T. Wang, H.J. Qi, Recycling of epoxy thermoset and composites via good solvent assisted and small molecules participated exchange reactions, ACS Sustain. Chem. Eng. 6 (2018) (2018) 9189–9197, https://doi.org/10.1021/acssuschemeng.8b01538.